

# Metal-Modified Nucleobase Sextet: Joining Four Linear Metal Fragments (*trans*-a<sub>2</sub>Pt<sup>II</sup>) and Six Model Nucleobases to an Exceedingly Stable Entity

Roland K. O. Sigel,<sup>[b]</sup> Susan M. Thompson,<sup>[c]</sup> Eva Freisinger,<sup>[d]</sup>  
Frank Glahé,<sup>[a]</sup> and Bernhard Lippert<sup>[a]\*</sup>

Dedicated to Professor Herbert Jacobs on the occasion of his 65th birthday

**Abstract:** Crosslinking of three different model nucleobases (9-ethyladenine, 9-EtA; 9-ethylguanine, 9-EtGH; 1-methyluracil, 1-MeU) by two linear *trans*-a<sub>2</sub>Pt<sup>II</sup> (a = NH<sub>3</sub> or CH<sub>3</sub>NH<sub>2</sub>) entities leads to a flat metal-modified base triplet, *trans,trans*-[(NH<sub>3</sub>)<sub>2</sub>Pt(1-MeU-*N*3)-(μ-9-EtA-*N*7,*N*1)Pt(CH<sub>3</sub>NH<sub>2</sub>)<sub>2</sub>(9-EtGH-*N*7)]<sup>3+</sup> (**4b**). Upon hemideprotonation of the 9-ethylguanine base at the *N*1 position, **4b** spontaneously dimerizes to

the metalated nucleobase sextet **5**, [(**4b**) ≡ (**4b**-H)]<sup>5+</sup>. In this dimeric structure a neutral and an anionic guanine ligand, which are complementary to each other, are joined through three H bonds and additionally by two H bonds

between guanine and uracil nucleobases. Four additional interbase H bonds maintain the approximate coplanarity of all six bases. The two base triplets form an exceedingly stable entity ( $K_D = 500 \pm 150 \text{ M}^{-1}$  in DMSO), which is unprecedented in nucleobase chemistry. The precursor of **4b** and several related complexes are described and their structures and solution properties are reported.

**Keywords:** hydrogen bonds • molecular recognition • nucleobases • platinum

## Introduction

Metal ions with a preference for linear or *trans*-square-planar coordination geometries such as Hg<sup>II</sup>,<sup>[1]</sup> Ag<sup>I</sup>,<sup>[2]</sup> and Cu<sup>II</sup><sup>[3]</sup> are among the earliest metal ions studied with regard to their complex formation properties with DNA, RNA, and homopolynucleotides. A major motivation of this past work was to understand the alterations of physicochemical properties, for example, UV spectra or viscosity of these macromolecules in the presence of the above metal ions. Subsequently phenomena such as DNA aggregation and formation of regularly metalated double-helical, as well as tetrastranded structures

have become a major focus of interest. X-ray crystallography of model compounds<sup>[4–6]</sup> and NMR spectroscopy<sup>[7]</sup> have greatly assisted in improving our understanding of these phenomena. Still, no conclusive picture of DNA crosslinking patterns with these metal ions is available at present. The enormous interest in the chemistry of cisplatin–DNA interactions following the discovery of its antitumor activity<sup>[8]</sup> may have contributed to this situation.

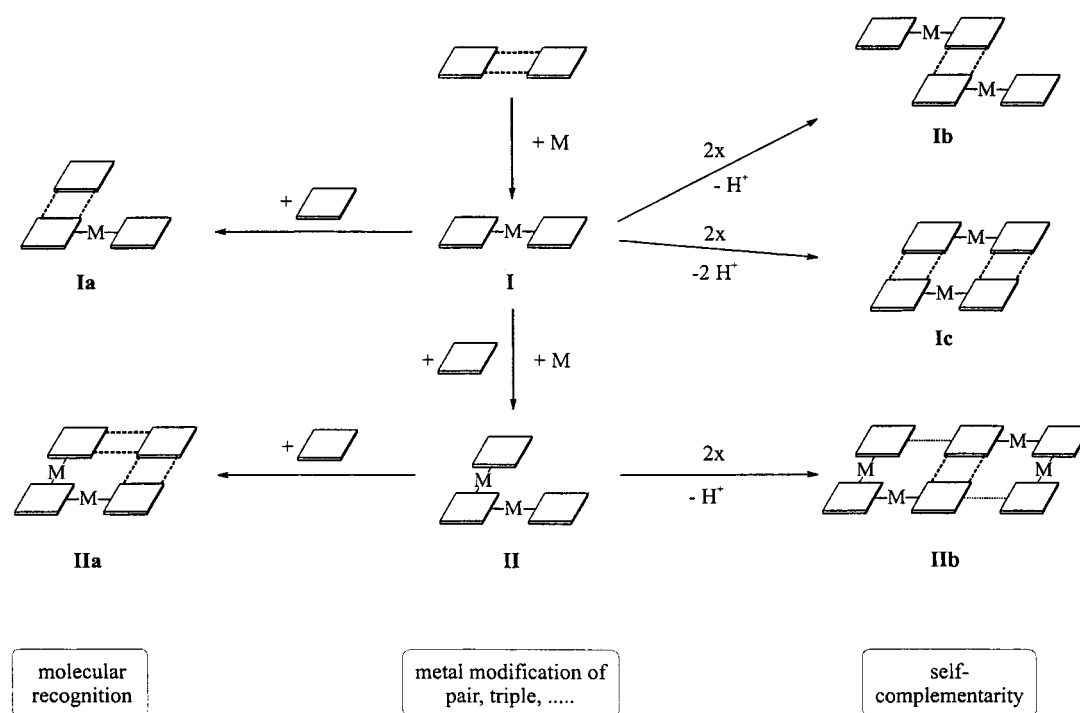
We have, initially with the aim of modeling DNA crosslinking reactions brought about by another linear metal entity, *trans*-a<sub>2</sub>Pt<sup>II</sup> (a = amine or ammine),<sup>[9]</sup> synthesized and structurally characterized a series of bisnucleobase complexes.<sup>[10]</sup> This work, carried out with kinetically inert Pt<sup>II</sup> species, was also considered to be relevant to the coordination chemistry of the aforementioned other linear metal entities, at least as far as structural aspects are concerned. The simple concept of replacing hydrogen bonds between nucleobases in a base pair by linear metal fragments (“metal-modified base pairs”)<sup>[11]</sup> has subsequently been extended to base triplets and base quartets.<sup>[12]</sup> In the course of these studies we observed that twofold metal coordination to *N*7 and *N*1 of purine bases generates 90° angles between the metal–*N* vectors,<sup>[12, 13]</sup> a feature facilitating formation of regularly shaped, flat nucleobase aggregates. Similarly, the 120° angle in dimetalated pyrimidine nucleobases, for example, between *M*–*N*3 and *M*–*C*5 vectors of cytosine, has been utilized to prepare a molecular hexagon.<sup>[14]</sup> We could further demonstrate that

[a] Prof. Dr. B. Lippert, F. Glahé  
Fachbereich Chemie, Universität Dortmund  
44221 Dortmund (Germany)  
Fax: (+49)231-755-3797  
E-mail: lippert@pop.uni-dortmund.de

[b] Dr. R. K. O. Sigel  
Department of Biochemistry and Molecular Biophysics  
Columbia University, Black Building, Room 513  
650 W 168th Street, New York, NY 10032 (USA)

[c] S. M. Thompson  
Institut für Anorganische Chemie, Technische Universität Wien  
Getreidemarkt 9/153, 1060 Wien (Austria)

[d] Dr. E. Freisinger  
Department of Pharmacological Sciences  
State University of New York at Stony Brook, Stony Brook  
NY, 11794 (USA)



Scheme 1. Strategy applied for the synthesis of a platinated nucleobase sextet **IIb** starting from a metalated nucleobase pair **I** (see also text). Other ways of molecular recognition are also indicated.

coordinative metal binding in combination with interbase H bonding leads to additional variations in the kind of aggregations.<sup>[15–19]</sup> In a number of cases unexpected H bonding patterns were observed, such as interguanine triple H bonding,<sup>[16]</sup> a reinforced Watson–Crick pairing scheme between guanine and cytosine,<sup>[17a, 19]</sup> a new base pairing scheme between guanine and cytosine,<sup>[17b]</sup> or H bonding involving an aromatic proton (H5) of a cytosine nucleobase and an imino group (N1) of a guanine base.<sup>[18]</sup> Mingos and co-workers

have adopted a similar approach and exploited the directional interactions of H bonds between metal coordination compounds in studies aimed at crystal engineering.<sup>[20]</sup>

Herein we report on a nucleobase sextet containing four *trans*- $a_2Pt^{II}$  fragments and multiple interbase H bonds, which was built in a stepwise fashion and proved to be exceedingly stable in solution.

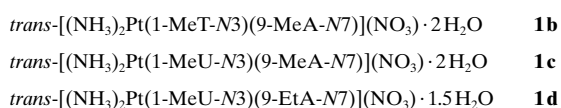
## Results and Discussion

**Formation strategy:** Scheme 1 provides the strategy applied for the formation of the nucleobase sextet **IIb**. Starting from the metalated base pair **I**, a dimetalated base triplet **II** was synthesized. As previously demonstrated for **I** and **II**, these complexes retain the ability of recognizing other bases, thereby forming metalated forms of base triplets (**Ia**<sup>[19, 21]</sup>) and base quartets (**IIa**<sup>[17a, 19]</sup>), respectively. On the other hand, from guanine-containing complexes **I** and **II**, self-complementary species (**Ib**,<sup>[16]</sup> **Ic**,<sup>[18]</sup> and **IIb**) can be generated upon semi- or full guanine deprotonation at the N1 position, followed by dimerization through H bond formation. This concept can be further extended to fully metalated nucleobase quartets (not shown). Outlined below is a description of the various precursor compounds for the synthesis of the nucleobase sextet.

**Mixed adenine, thymine (uracil) precursors:** We have previously reported the crystal structure of *trans*- $[(NH_3)_2Pt(1-MeT-N3)(9-MeA-N7)](ClO_4) \cdot 2.5H_2O$  (**1a**; 1-MeT = 1-methylthymine; 9-MeA = 9-methyladenine),<sup>[11]</sup> and now present

**Abstract in German:** Die Verknüpfung dreier unterschiedlicher Modellnucleobasen (9-Ethyladenin, 9-EtA; 9-Ethylguanin, 9-EtGH; 1-Methyluracilat, 1-MeU) über zwei lineare *trans*- $a_2Pt^{II}$ -Einheiten ( $a = NH_3$  oder  $CH_3NH_2$ ) führt zu einem flachen metall-modifizierten Basentriplett, *trans,trans*- $[(NH_3)_2Pt(1-MeU-N3)(\mu-9EtA-N7,N1)Pt(CH_3NH_2)_2(9-EtGH-N7)]^{3+}$  (**4b**). **4b** dimerisiert im Falle einer Hemi-Deprotonierung der Guanin-N1 Position spontan zu einem Nucleobasen-Sextett **5**,  $[(4b) \equiv (4b-H)]^{5+}$ . Die beiden Triplett-Strukturen werden hierbei über 3 H-Brücken zwischen den komplementären Guaninbasen sowie über zwei H-Brücken zwischen jeweils einem Guanin- und einem Uracilliganden verknüpft. Vier weitere H-Brücken zwischen Guanin und Adenin sowie zwischen Adenin und Uracil führen zu annähernder Coplanarität aller sechs Basen. Die Komplexbildung der beiden Basentriplets ist mit  $K_D = 500 \pm 150 \text{ M}^{-1}$  (DMSO) so hoch wie in keinem anderen bekannten Nucleobasenassoziat. Im folgenden werden ferner die Strukturen und das Lösungsverhalten der Vorstufe von **4b** sowie mehrerer verwandter Verbindungen diskutiert.

the preparation and structural characterization of three closely related species, **1b–1d** (9-EtA = 9-ethyladenine,



1-MeU = 1-methyluracilate). Apart from being precursors of the type of compounds described below, we were particularly interested in the association behavior of these compounds in the solid state and in solution. Having observed the association of two  $\text{trans}[(\text{NH}_3)_2\text{Pt}(1\text{-MeC-N3})(9\text{-EtG-N7})]^+$  ions (1-MeC = 1-methylcytosine; 9-EtG = 9-ethylguanine) to a dimetalated base quartet and specifically formation of  $\text{CH} \cdots \text{N}$  hydrogen bonds (Figure 1a),<sup>[18]</sup> we reasoned that with

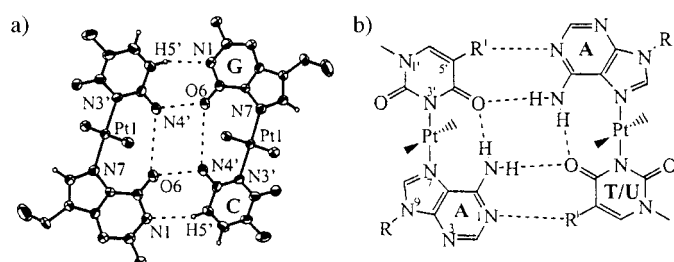


Figure 1. Quartet formation upon dimerization as observed in the crystal structure of  $\text{trans}[(\text{NH}_3)_2\text{Pt}(1\text{-MeC-N3})(9\text{-MeG-N7})]^+$  (a),<sup>[18b]</sup> and as anticipated for complexes **1a–1d** (b). R = Me, Et, R<sup>1</sup> = H, Me.

mixed 1-MeT (1-MeU)/9-RA compounds an analogous association pattern could be realized (Figure 1b; 9-RA = 9-alkyladenine), possibly depending on factors such as counteranions and water content. We were aware that  $\text{CH} \cdots \text{N}$  hydrogen bonds are generally rare and weak, and that there is a difference between the previously observed case and the one studied here: It refers to the sequence of donor (D) and acceptor (A) sites in the two compounds, being AADD in the case of the mixed guanine, cytosine complex, yet ADAD in the mixed adenine, thymine (uracil) compounds. To summarize, **1a–1d** do not form base quartets of the type shown in Figure 1b, either in solution ( $[\text{D}_6]\text{DMSO}$ ) or in the solid state. The solubilities of **1a–1d** did not permit solution studies in solvents of poorer H bonding capacities. Thus, although self-complementary in principle, the AADD sequence, not unexpectedly is more favorable for interbase H bond formation, possibly due to secondary electrostatic interactions.<sup>[20a, 22]</sup>

Details concerning the crystals, the X-ray measurement, and the refinement of the data are listed in Table 1. Table 2 provides a few selected structural details of the new compounds **1b–1d**. All four complexes form an intramolecular hydrogen bond between the exocyclic amino group  $\text{N6H}_2$  of the adenine moiety and either  $\text{O2}'$  or  $\text{O4}'$  of the pyrimidine ligand (Figure 2). This distance is slightly longer than normally expected in one of the two independent cations of **1a** (3.15(1) Å, cation 1)<sup>[11]</sup> and in the other thymine compound **1b** (3.238(7) Å; 3.08(1)–3.09(2) Å in **1a** (cation 2), **1c**, and **1d**). However, in each case it follows a distortion of the

Table 1. Crystallographic data for compounds **1b**, **1c**, **1d**, **2a**, **4a**, and **5**.

	<b>1b</b>	<b>1c</b>	<b>1d</b>	<b>2a</b>	<b>4a</b>	<b>5</b>
formula	$\text{C}_{12}\text{H}_{24}\text{N}_{10}\text{O}_7\text{Pt}$	$\text{C}_{11}\text{H}_{22}\text{N}_{10}\text{O}_7\text{Pt}$	$\text{C}_{12}\text{H}_{23}\text{N}_{10}\text{O}_{6.5}\text{Pt}$	$\text{C}_{14}\text{H}_{32}\text{N}_{11}\text{O}_{11}\text{Cl}_3\text{Pt}_2$	$\text{C}_{21}\text{H}_{49.4}\text{N}_{16}\text{O}_{20.2}\text{Cl}_3\text{Pt}_2$	$\text{C}_{42}\text{H}_{82}\text{N}_{32}\text{O}_{28.5}\text{Cl}_3\text{Pt}_4$
formula weight [g mol <sup>-1</sup> ]	615.5	601.48	606.49	1026.99	1345.9	1224.5
crystal color and habit	colorless blocks	colorless plates	colorless triangles	colorless blocks	colorless triangles	colorless sticks
crystal size [mm]	0.39 × 0.37 × 0.20	0.25 × 0.25 × 0.19	0.29 × 0.11 × 0.11	0.50 × 0.18 × 0.13	0.25 × 0.25 × 0.06	0.25 × 0.13 × 0.13
T [K]	293(2)	293(2)	293(2)	293(2)	193(2)	293(2)
λ [Å]	0.71069	0.71069	0.71069	0.71069	0.71069	0.71069
crystal system	monoclinic	triclinic	orthorhombic	monoclinic	monoclinic	monoclinic
space group	$P2_1/n$	$P\bar{1}$	$Pccn$	$C2/c$	$P2_1/c$	$P2/c$
a [Å]	8.950(2)	9.110(2)	22.486(4)	11.455(2)	12.648(3)	17.212(3)
b [Å]	21.641(4)	10.901(2)	25.984(5)	20.392(4)	31.564(6)	17.551(4)
c [Å]	11.167(2)	11.099(2)	7.278(1)	26.505(5)	12.188(2)	15.656(3)
α [°]		97.22(3)				
β [°]	111.43(3)	108.96(3)		99.35(3)	113.63(3)	114.45(3)
γ [°]		92.09(3)				
V [Å <sup>3</sup> ]	2013.4(7)	1030.6(3)	4252.4(13)	6109.1(20)	4457.7(15)	4305.4(15)
Z	4	2	8	8	4	4
ρ <sub>calcd</sub> [g cm <sup>-3</sup> ]	2.013	1.938	1.895	2.233	2.005	1.889
μ(MoKα) [mm <sup>-1</sup> ]	7.028	6.862	6.652	9.479	6.539	6.721
F(000)	1200	584	2360	3904	2624	2366
2θ range [°]	4.3 ≤ 2θ ≤ 52.5	6.3 ≤ 2θ ≤ 48.3	5.0 ≤ 2θ ≤ 49.5	9.2 ≤ 2θ ≤ 51.3	3.5 ≤ 2θ ≤ 54.5	4.6 ≤ 2θ ≤ 41.8
reflections collected	4880	2009	12578	10614	17645	8013
reflections independent	4601 ( $R_{\text{int}} = 0.029$ )	2009 ( $R_{\text{int}} = 0.047$ )	3481 ( $R_{\text{int}} = 0.087$ )	5444 ( $R_{\text{int}} = 0.052$ )	9423 ( $R_{\text{int}} = 0.122$ )	4389 ( $R_{\text{int}} = 0.107$ )
reflections observed	3432 ( $I \geq 2\sigma(I)$ )	1298 ( $I \geq 2\sigma(I)$ )	1802 ( $I \geq 2\sigma(I)$ )	3521 ( $I \geq 2\sigma(I)$ )	3783 ( $I \geq 2\sigma(I)$ )	1668 ( $I \geq 2\sigma(I)$ )
refined parameters	284	186	259	389	537	259
extinction coefficient	–	–	–	–	–	$2.4(5) \times 10^{-4}$
$R_1^{[a]}$ (obs. data)	0.0353	0.0567	0.0479	0.0306	0.0508	0.0589
$wR_2^{[b]}$ (obs. data)	0.0764	0.1250	0.0877	0.0531	0.0787	0.1164
GoF	1.094	1.095	1.188	1.004	1.068	1.122

[a]  $R_1 = \sum |F_o| - |\sum |F_c|| / \sum |F_o|$ . [b]  $wR_2 = [\sum w(F_o^2 - F_c^2)^2 / \sum w(F_o^2)]^{1/2}$ .

Table 2. Comparison of selected bond lengths [Å], hydrogen-bond lengths [Å], angles [°], and angles between pyrimidine/adenine planes [°] in the complexes **1b–d**.

	<b>1b</b>	<b>1c</b>	<b>1d</b>
Pt–N7	2.015(5)	2.01(1)	2.01(1)
Pt–N3'	2.018(5)	2.01(1)	1.99(1)
Pt–N10	2.043(5)	2.03(1)	2.011(8)
Pt–N11	2.051(5)	2.04(1)	2.047(8)
N7–Pt–N3'	176.0(2)	173.9(7)	172.7(4)
N10–Pt–N11	179.1(2)	177.3(8)	178.5(3)
N7–Pt–N10	90.9(2)	89.7(5)	91.0(4)
N7–Pt–N11	89.7(2)	90.3(5)	90.0(3)
N3'–Pt–N10	90.0(2)	89.8(9)	88.8(3)
N3'–Pt–N11	89.4(2)	90.4(6)	90.5(3)
Pt–N7–C5	126.5(4)	126(1)	127.2(8)
Pt–N7–C8	128.1(4)	129(1)	129.4(9)
Pt–N3'–C2'	120.6(4)	115(1)	115.7(8)
Pt–N3'–C4'	115.9(6)	122(2)	124.0(9)
N11...O(pym) <sup>[a]</sup>	2.954(7)	2.96(2)	2.93(1)
N10...O(pym) <sup>[a]</sup>	–	–	2.99(1)
N6...O(pym) <sup>[b]</sup>	3.238(7)	3.09(2)	3.08(1)
N10...N1	3.054(8)	3.11(2)	3.24(1)
N11...N1	–	–	3.22(1)
N11...N3'	–	3.12(2)	–
pym/adenine	6.1(3)	11.2(8)	14.3(2)

[a] Intermolecular H bonds, O2' in **1b**, O4' in **1c** and **1d**. [b] Intramolecular H bonds, O4' in **1b**, O2' in **1c** and **1d**.

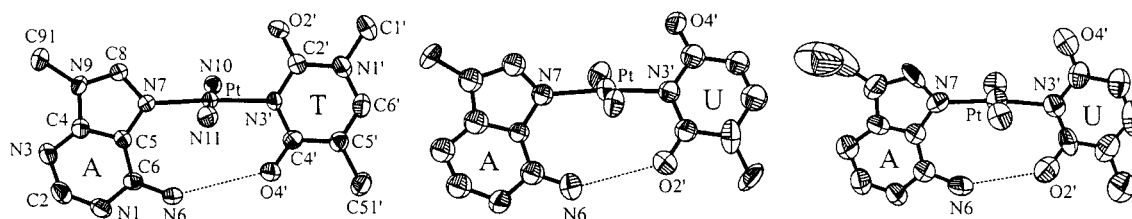


Figure 2. Cations of the complexes **1b** (left), **1c** (center), and **1d** (right) together with their atomic numbering schemes. Anions and water molecules found in the crystal structure are omitted for clarity. The ellipsoids are drawn at 50% probability.

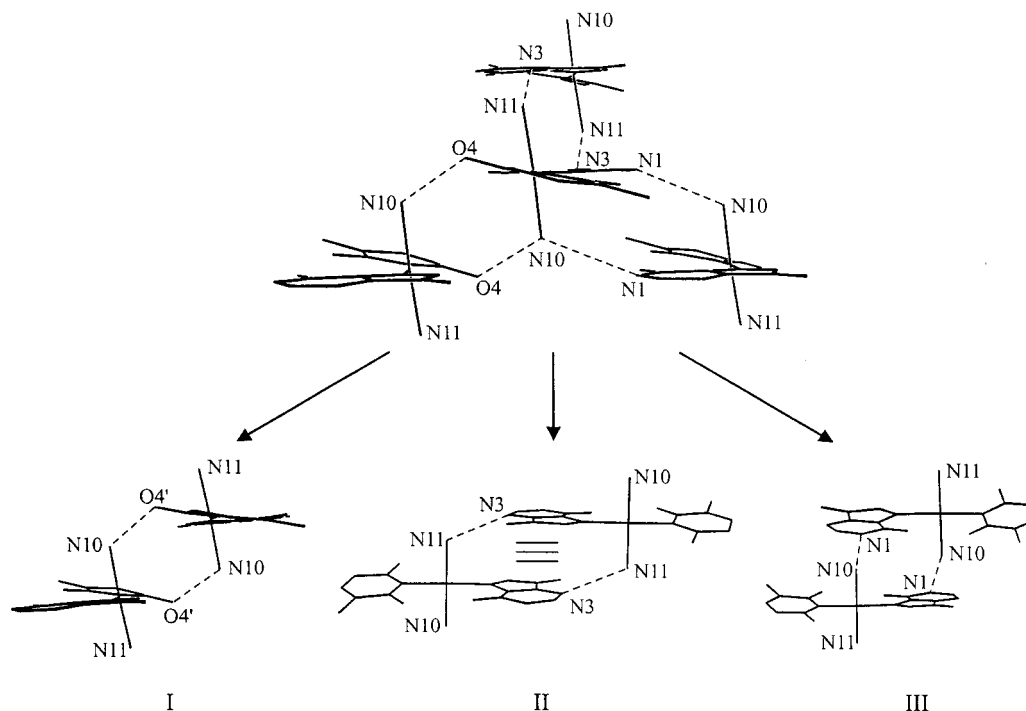


Figure 3. Dimers of types I, II, and III found in the crystal structure of compound **1c** (see text for details).

platinum coordination sphere, that is  $N7 - Pt - N3'$  is always  $< 180^\circ$  on the side facing the intramolecular H bond. These intramolecular hydrogen bonds also have an effect on the coordination angles at N7 of the adenine and N3' of the pyrimidine ligands; those  $Pt - N7/N3' - C$  angles facing the intramolecular  $N6H_2 \cdots O2'/4'$  bond are always significantly smaller than the ones on the opposite side. The dihedral angle between the nucleobases is between  $4.5^\circ$  (in one cation of **1a**)<sup>[11]</sup> and  $14.3(2)^\circ$  in **1d**.

As mentioned above, none of these complexes form a planar quartet through dimerization. Nevertheless, several other forms of dimers are formed through hydrogen bonding and stacking, as shown in Figure 3 for complex **1c**. The most common feature found in all four complexes, is that of dimers (type I) with two complexes connected through two H bonds between the ammine ligands and O2' or O4', respectively (lengths of H bonds between 2.87(1) Å (**1a**), and 2.96(2) Å (**1c**); see also Figure 3). This pattern resembles the one described for transplatinum complexes with two pyrimidine ligands or one pyrimidine and one 7,9-dimethylguanine moiety,<sup>[23]</sup> although in these cases four hydrogen bonds are formed as a consequence of the nature of the ligands. In compounds **1a**, **1c**, and **1d** it is the carbonyl oxygen not involved in the

intramolecular bond with N6H<sub>2</sub>, which forms this contact to the adjacent complex, whereas in **1b** O4' is involved in both the intra- and the intermolecular hydrogen bond.

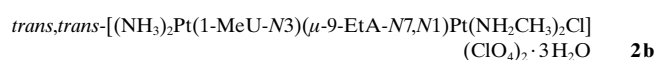
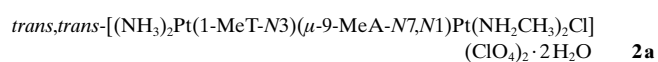
Another pattern of dimerization involves two hydrogen bonds between an ammine group of the transplatinum centers and either N3 (type II) or N1 (type III) of the adenine moieties (Figure 3). All hydrogen bonds involved in these patterns are between 3.00(1) (**1a**) and 3.24(1) Å (**1d**). A dimer of type II (NH<sub>3</sub>⋯N3) is only found in compound **1c**, whereas dimers of type III (NH<sub>3</sub>⋯N1) are formed between cations of **1b**, **1c**, and **1d**. Compound **1a** adopts a mixed conformation, dimerizing through a NH<sub>3</sub>⋯N3 (3.00(1) Å) as well as a NH<sub>3</sub>⋯N1 hydrogen bond (3.18(1) Å). In addition, dimer formation is reinforced by a stacking interaction (3.3 Å) between the two adenine moieties. This stacking interaction is very similar to the one found in type II of **1c** (Figure 3) or type III of **1d**. In **1b**, stacking is observed between the adenine moiety and the nitrate anion (3.2 Å).

Concentration-dependent <sup>1</sup>H NMR measurements have been performed in [D<sub>6</sub>]DMSO solution with **1b**, **1c**, and **1d**. Despite the fact that all complexes carry an overall charge of +1 (as in the case of *trans*-[(NH<sub>3</sub>)<sub>2</sub>Pt(1-MeC-N3)(9-EtG-N7)]<sup>+</sup>)<sup>[18]</sup> and two of them have an aromatic H5' proton (and not a methyl group), none displays a concentration dependence of any proton resonance. Hence no evidence for a quartet association in solution could be detected.

In [D<sub>6</sub>]DMSO a singlet for C51'H<sub>3</sub> in **1b**, or a doublet for H5' in **1c** and **1d**, respectively, is observed. In contrast, in D<sub>2</sub>O the H5' resonances are doubled (δ = 5.76, Δδ = 0.02) suggesting the existence of two uracil rotamers. Water, being a proton donor as well as an acceptor, can form hydrogen bonds simultaneously to the amino group of adenine and to O2' (or O4') of uracil/thymine. As a consequence, rotation of 1-MeU about the Pt–N3' bond is expected to be slower. In contrast, DMSO acts only as a proton acceptor and consequently can only bind to N6H<sub>2</sub>. Thus, DMSO is expected not to stabilize a particular rotamer and base rotation will therefore be less hindered than in water. Consequently, if rotation is fast on the NMR time scale only an averaged signal in the <sup>1</sup>H NMR spectrum is observed. It is feasible that such a rotation will be a handicap for dimerization.

In the <sup>195</sup>Pt NMR spectra of complexes **1c** and **1d**, no doubling of the resonance is observed. This is not surprising because the chemical environment of the Pt<sup>II</sup> center does not change with the rotation of the uracil ligand about the Pt–N3' bond. However, there have been cases where distinctly different signals due to rotamers have been observed.<sup>[24]</sup>

**Intermediate complexes:** Complexes **1b** and **1d** were allowed to react with an excess of *trans*-[(CH<sub>3</sub>NH<sub>2</sub>)<sub>2</sub>PtCl<sub>2</sub>] to give **2a** and **2b** in 75 and 61% yield, respectively. Crystals of **2a** suitable for X-ray structure determination were obtained by recrystallization from water and slow evaporation at room temperature.



Complex **2a** crystallizes in the space group *C2/c* (Table 1). X-ray crystallography reveals one water molecule spread over two positions with occupancies of 75 and 25%, respectively. Selected bond lengths and angles are listed in Table 3. The

Table 3. Comparison of selected bond lengths [Å], hydrogen bonds [Å], dihedral angles [°], and angles between different nucleobase/nucleobase planes [°] in the crystal structures of complexes **2a**, **4a**, and **5**.

	<b>2a</b>	<b>4a</b>	<b>5</b>
Pt1–N3'	2.016(5)	2.013(7)	2.03(2)
Pt1–N7	2.001(5)	2.028(8)	2.01(2)
Pt2–N1	2.028(5)	2.041(8)	2.02(2)
Pt2–N7g <sup>[a]</sup>	2.293(2)	2.009(8)	1.94(2)
N6⋯O2'/O4' <sup>[b]</sup>	2.883(7)	3.13(1)	3.35(3)
N6a⋯O6g	–	3.019(9)	3.17(2)
N7–Pt1–N3'	171.7(2)	173.3(8)	176.9(9)
N1–Pt2–N7g <sup>[a]</sup>	178.9(2)	172.9(3)	176.6(9)
Pt1–N3'–C2'	114.8(5)	120.6(7)	119(3)
Pt1–N3'–C4'	124.0(5)	114.9(7)	121(2)
Pt1–N7–C5	122.3(4)	126.3(6)	125(2)
Pt1–N7–C8	132.1(4)	127.8(8)	128(2)
Pt2–N1–C2	117.5(4)	119.7(7)	119(2)
Pt2–N1–C6	122.3(4)	118.5(6)	121(2)
Pt2–N7g–C5g	–	121.4(7)	127(2)
Pt2–N7g–C8g	–	133.2(7)	132(2)
pym/A	11.9(2)	17.0(4)	7.6(9)
A/G	–	17.4(3)	10.4(6)
pym/G	–	34.2(4)	3(1)

[a] In case of complex **2a** this bond length refers to Pt2–Cl and the angle to N1–Pt2–Cl. [b] O2' or O4' in **2a** and **5**, O4' in **4a**.

cations are connected through intermolecular hydrogen bonds between O4' and one of the amine groups of the monochloroplatinum center (2.805(7) Å) to form infinite chains as shown in Figure 4. A short intramolecular hydrogen

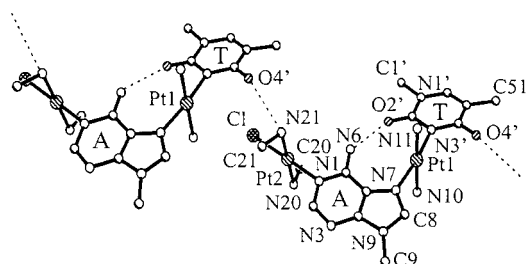


Figure 4. Two cations of **2a** together with their atomic numbering scheme and some intra- and intermolecular hydrogen bonds. Anions and water molecules are omitted for clarity.

bond between O2' of thymine and N6H<sub>2</sub> of adenine (2.883(7) Å) correlates to an angle of 171.7(2)° for N3'–Pt1–N7, which is noticeably smaller than the ideal angle of 180°. Since no such intramolecular hydrogen bond can be formed at the second platinum center (Pt2), the angle at this site is virtually undistorted (179.5(2)°). A further consequence of this intramolecular hydrogen bond is the reduction of external ring angles at the platinum coordination sites of thymine–N3' (Pt1–N3'–C2' 114.8(5)°) and adenine–N7 (Pt1–N7–C5 122.3(4)°) facing the hydrogen bond, whereas the bond angles

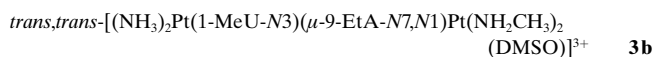
at the outer side increase (Pt1-N3'-C4' 124.0(5)° and Pt1-N7-C8 132.1(4)°).

Owing to the described distortion at the N7 coordination site of the adenine moiety, the angle formed between the two platinum vectors N1-Pt2 and Pt1-N7 at the adenine is only 82.8(8)°. It is thus significantly smaller than the corresponding angle in the diplatinated cation  $\{trans-[(CH_3NH_2)_2PtCl]_2(\mu-9-MeA-N1,N7)\}^{2+}$  (87.9(4)°),<sup>[12c]</sup> where the thymine ligand in **2a** is replaced by a chloro ligand.

It was not possible to unambiguously determine which rotational isomer of the thymine ligand is preferred in the solid state, that is, whether O2' or O4' forms the intramolecular hydrogen bond with N6H<sub>2</sub>. This is due to the pseudo-twofold axis through N3' and C6' of the thymine base and the very similar chemical environments of the C5'-CH<sub>3</sub> and the N1'-CH<sub>3</sub> groups, which makes a differentiation of C5' and N1' difficult. Both rotamers have been refined but gave identical *R* values and similar atomic displacement factors for N1' and C5', respectively. Therefore it is quite possible that in the solid state both rotamers are present in a 1:1 ratio. We note that even with the unplatinated Hoogsteen pair between 9-ethyladenine and 1-methylthymine a similar disorder occurs, leading to the reversed Hoogsteen pair.<sup>[25]</sup>

**Solution studies of 2a and 2b:** As previously observed for complexes **1c** and **1d**, the <sup>1</sup>H NMR spectra of **2a** and **2b** in D<sub>2</sub>O indicate hindered rotation of the pyrimidine moiety around the Pt1-N3' bond, suggesting the existence of the intramolecular hydrogen bond between O2'/O4' and N6H<sub>2</sub>, or again simultaneous H binding of a water molecule to O2'/O4' and N6H<sub>2</sub>. Thus, resonances of the N1'-CH<sub>3</sub> and H5' or C5'-CH<sub>3</sub>, respectively, are both split in a 6:4 ratio, differing by about 0.03 ppm (**2a**) or 0.04 ppm (**2b**). All the other resonances, that is, especially H6' of the pyrimidine ligand, but also all of the adenine protons, show no doubling. Again, as for complexes **1b–1d**, no indication for rotamers can be observed in DMSO solution.

In all solvents used (D<sub>2</sub>O, [D<sub>7</sub>]DMF, and [D<sub>6</sub>]DMSO), the <sup>195</sup>Pt NMR spectra of **2a** and **2b** unexpectedly showed only a single broad peak at  $\delta = -2470$  (**2a**) or  $-2461$  (**2b**). In [D<sub>6</sub>]DMSO, however, a second peak evolved within an hour at  $\delta = -3169$  (**2a**) ( $\delta = -3173$ ; **2b**) (Figure 5). The reaction was complete after twelve hours. The latter resonance is assigned to **3b**. [dienPt(9-EtGH-N7)]<sup>2+</sup> was used as platinum reference ( $\delta = -2765$ ).



It is difficult to be sure whether the peak at  $\delta = -2461$  diminishes during the reaction, that is, if the two platinum resonances in **2b** are really superimposed by coincidence. Alternatively, there could be a broadening of the Pt2 resonance in **2a** or **2b** due to rapid relaxation.<sup>[26]</sup> Support in favor of the first explanation comes from a comparison of <sup>195</sup>Pt chemical shifts of **1c** (PtN<sub>4</sub> coordination sphere) and  $trans-[(NH_3)_2Pt(7,9-DimeG-N1)Cl]^+$  (PtN<sub>3</sub>Cl coordination sphere): Both shifts are remarkably similar;  $\delta = -2466$  (**1c**) and

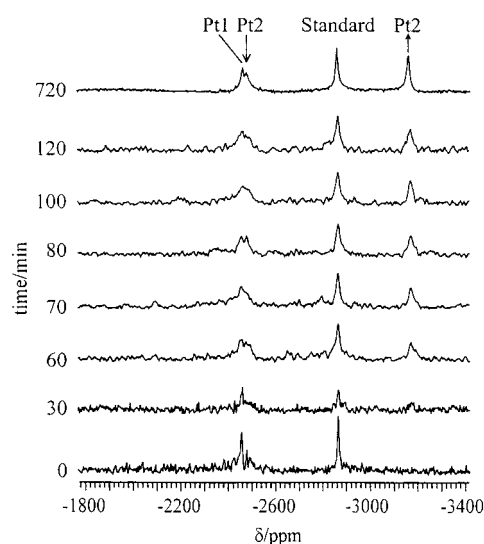
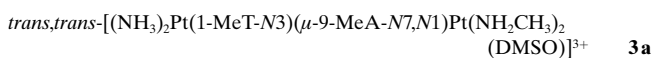


Figure 5. Time course of the chloro ligand exchange in **2b** by a solvent molecule, giving **3b**, as seen in <sup>195</sup>Pt NMR spectra in [D<sub>6</sub>]DMSO. The standard refers to the signal of [dienPt(9-EtGH-N7)]<sup>2+</sup> ( $\delta = -2765$ ).

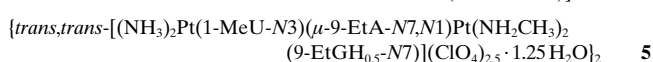
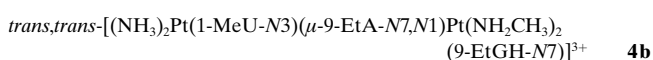
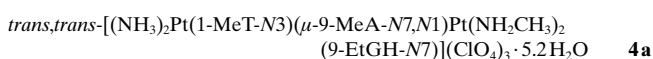
$-2458$ . Hence, substitution of a negatively charged chloro ligand by a N3' deprotonated pyrimidine ligand appears not to have much effect on the <sup>195</sup>Pt resonance. In contrast, Pt<sup>II</sup> centers with four neutral ligands are normally found at higher field.<sup>[27]</sup>

Complex **2a** behaves identically with respect to the <sup>195</sup>Pt NMR spectra and the exchange of the chloro ligand by a [D<sub>6</sub>]DMSO solvent molecule to give the cation **3a**.



In the <sup>1</sup>H NMR spectra, all the chemical shifts change dramatically upon replacing the chloro ligand by a DMSO molecule. For example, in complexes **3a** and **3b**, the resonances of the CH<sub>3</sub>NH<sub>2</sub> group at Pt2 are both shifted downfield by about 0.15 ppm (NH<sub>2</sub>) and 0.25 ppm (CH<sub>3</sub>) compared to the chloro species. All other resonances are shifted to higher field. It is not surprising that the aromatic protons of the adenine moiety H2 and H8 are affected most, by 0.33 and 0.48 ppm in **3a** and 0.35 and 0.54 ppm in **3b**, respectively. The aliphatic protons and the protons of the pyrimidine ligand are shifted upfield in both DMSO complexes between 0.09 and 0.04 ppm (for the detailed chemical shifts of all species see Experimental Section).

**Platinated nucleobase triplet:** Reaction of the bisnucleobase complexes **2a** and **2b** with 9-EtGH yielded **4a** and **4b**. The latter could only be obtained in acidic solution and could not be isolated, as always the hemideprotonated sextet **5** formed.



Crystals of **4a** suitable for X-ray crystallography were obtained upon recrystallization from aqueous solution and slow evaporation at 4 °C. Complex **4a** crystallized in the space group  $P2_1/c$  (see Table 1 for further details) with three perchlorate anions and 5.2 water molecules, of which four positions are fully occupied and the remaining 1.2 water molecules are distributed over three positions with occupancy factors of 0.6, 0.4, and 0.2. A view of the cation is shown in Figure 6 and a selection of the most important bond lengths,

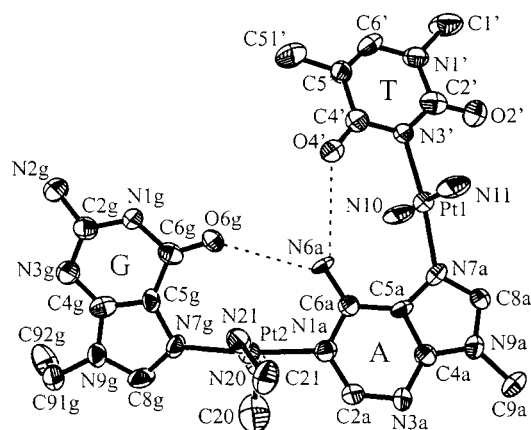


Figure 6. Cation of **4a** together with its atomic numbering scheme. The anions are omitted for clarity. The ellipsoids are drawn at 50% probability.

angles and hydrogen bonds is listed in Table 3. Both  $Pt^{II}$  centers have an approximately square planar geometry with  $Pt-N$  bond lengths in the normal range (2.009(8)–2.055(8) Å).

As discussed previously for complex **2a**, both possible rotamers have been refined and the one giving the better  $R$  values and the more reasonable displacement factors for  $N1'$  and  $C5'$  was accepted. In this case  $O4'$  is involved in intramolecular hydrogen bonding with the exocyclic amino group of the adenine ligand (3.13(1) Å), very much as in the thymine-containing complex **1b**, yet in contrast to **1c** and **1d**, where  $O2'$  forms this hydrogen bond (in **2a** it can either be  $O2'$  or  $O4'$ ). Although this hydrogen bond is longer in **4a** than in the three complexes just mentioned, its existence is corroborated by the geometry about  $Pt1$  ( $N3'-Pt1-N7$  173.8(3)°;  $Pt1-N3'-C4'$  114.9(7)°;  $Pt1-N3'-C2'$  120.6(7)°). On the other hand, the opposite angles at the adenine moiety  $Pt1-N7a-C5a$  (126.3(6)°) and  $Pt1-N7a-C8a$  (127.8(8)°) are identical within the error limits.

As can be seen in Figure 6, the exocyclic amino group of the adenine moiety is involved in a second intramolecular hydrogen bond with  $O6g$  of 9-ethylguanine (3.019(9) Å). This H bond also leads to a distortion at the platinum center involved ( $N7g-Pt2-N1a$  (172.9(3)°). Again the angles at the coordinating  $N1a$  position of adenine are identical within the error limits ( $Pt2-N1a-C2a$  119.7(7)° and  $Pt2-N1a-C6a$  118.5(6)°) and thus do not contribute to the shortening of this hydrogen bond. In contrast, the angle  $Pt2-N7g-C5g$  in the guanine moiety that faces the intramolecular H bond, is significantly smaller (121.4(7)°) than the one on the opposite site ( $Pt2-N7g-C8g$  133.2(7)°).

The  $N1,N7$ -diplatinated adenine ligand forms a corner angle of 83.0(3)° which is about the same as found in **2a** (82.8(1)°). This is in good agreement with various quartet structures, which consist of adenine and guanine nucleobases and  $trans-a_2Pt^{2+}$  units, where angles are between 80.8(4)° and 91.6(4)°.<sup>[12a]</sup> The X-ray structure of the related nucleobase quartet  $\{trans,trans-[(NH_3)_2Pt(1-MeU-N3)(\mu-9-EtA-N7,N1)-Pt(CH_3NH_2)_2(9-EtGH-N7)=(1-MeC)]_2[1-MeC\equiv 1-MeCH](ClO_4)_{4.5}(NO_3)_{2.5}\cdot 8.7H_2O$  with two independent quartet structures reveals angles of 82.5(6)° and 86.2(9)°.<sup>[17a]</sup>

Two cations of **4a** interact through *head-to-tail* stacking of two 9-ethylguanines (3.36 Å apart; Figure 7 top). The two bases are exactly parallel since they are related by an

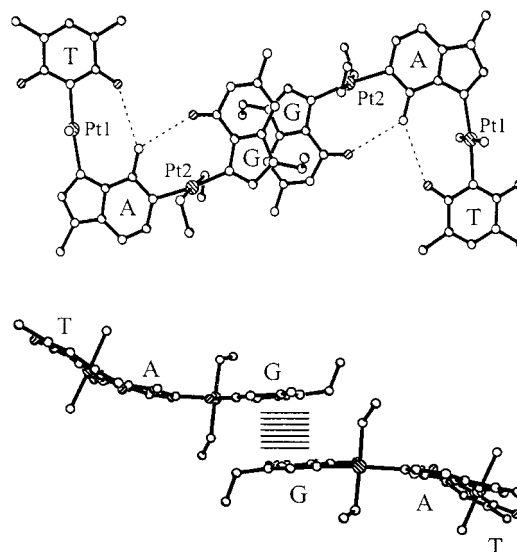


Figure 7. Head-to-tail stacking of two 9-ethylguanine ligands as observed in the solid-state structure of **4a**. View from the top (top) and from the side (bottom). The cations adopt the shape of a shallow bowl.

inversion center between the two nucleobase planes. This stacking interaction is the only contact between two neighboring cations, so no direct hydrogen bonding is observed. All donor and acceptor sites of the complexes, especially the different am(m)ine groups at the  $Pt^{II}$  centers and  $NH_2$  of 9-EtGH, are occupied by water molecules and oxygen atoms of the perchlorate anions. All hydrogen bond lengths are within the normal range (2.86(1)–3.25(1) Å), although one between a water molecule and the  $N1H$  of 9-ethylguanine is markedly shorter (2.75(1) Å).

Figure 7 also shows that the nucleobase triplet is not planar; both angles between the guanine and adenine planes and between the adenine and the thymine planes are in the same order (17.4(3)° and 17.0(4)°) and orientated in the same direction. Thus, the angle between 9-EtGH and 1-MeT adds up to 34.2(4)°, providing the impression of a shallow bowl formed by the base triplet.

**Solution studies of 4a and 4b:** Whereas NMR investigations of **4b** have been performed in  $D_2O$  only, **4a** has also been examined in  $[D_6]DMSO$ . To ensure full deuteration of the guanine  $N1$  position, all NMR spectra in  $D_2O$  have been

recorded at slightly acidic pH. Assignments of H8 of 9-EtGH and H8 and H2 of the adenine ligand as well as of the two platinum resonances in each of the two complexes have been achieved by  $^1\text{H}/^{195}\text{Pt}$  HMQC experiments.

Concerning the rotation of the pyrimidine ligand about the Pt1–N3' axis, both complexes **4a** and **4b** behave as discussed above for **1a–1d**. In  $\text{D}_2\text{O}$  a doubling of the alkyl resonances at the C1' and C5' positions is observed, whereas in  $[\text{D}_6]\text{DMSO}$  only a single set of signals is seen (see above).

The hydrogen bonding behavior of **4a** towards 1-methylcytosine in  $[\text{D}_6]\text{DMSO}$  and the determination of the stability constant of the resulting quartet (through concentration-dependent chemical shift measurements), where the cytosine moiety is bound in a Watson–Crick fashion to the guanine ligand, have been published earlier.<sup>[28]</sup>

**Determination of  $\text{p}K_{\text{a}}$  values:** The  $\text{p}K_{\text{a}}$  values of complexes **1c**, **4a**, and **4b** have been determined by using pH-dependent  $^1\text{H}$  NMR measurements in  $\text{D}_2\text{O}$  ( $20^\circ\text{C}$ ;  $I=0.1\text{ M}$ ,  $\text{NaNO}_3$ ).

In the pH range from 2 to 12, the pD-dependent chemical shift measurements of complex **1c** show only one acid–base equilibrium, which refers to the protonation of the N1 site of the adenine ligand (Figure 8a). The resonances of the uracil moiety are virtually unaffected by the change in pH, thus ruling out any acid–base equilibria involving this ligand.

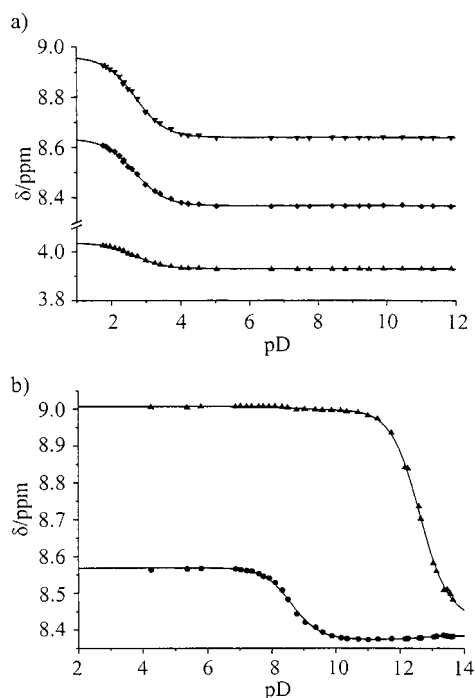


Figure 8. a) pH-dependent chemical shifts of complex **1c** in  $\text{D}_2\text{O}$  in the pD range from 1 to 12. The resonances H2 (▼), H8 (■) and  $\text{CH}_3$  (▲) of the adenine residue are shown (from top to bottom); b) pD-dependent chemical shifts of H2 from 9-EtA (▼) and H8 from 9-EtGH (●) of **4b** in the pD range from 4 to 14.

The changes in chemical shifts of all non-exchangeable protons of the adenine resonances were evaluated with a nonlinear least-squares fit after Newton–Gauss<sup>[28, 29]</sup> to give three  $\text{p}K_{\text{a}}^*$  values which hold for a  $\text{D}_2\text{O}$  solution (Table 4).

Table 4. Chemical shifts of the 9-methyladenine protons for the N1-protonated ( $\delta_{\text{NbH}}$ ) and deprotonated forms ( $\delta_{\text{Nb}}$ ) of **1c** as determined in  $\text{D}_2\text{O}$  ( $20^\circ\text{C}$ ;  $I=0.1\text{ M}$ ,  $\text{NaNO}_3$ ) from the experiment shown in Figure 8.<sup>[a]</sup>

	$\delta_{\text{NbH}}$	$\delta_{\text{Nb}}$	$\Delta\delta_1$	$\text{p}K_{\text{a}}^*$
	ppm			
H2	$8.961 \pm 0.003$	$8.639 \pm 0.001$	$0.322 \pm 0.003$	$2.697 \pm 0.015$
H8	$8.634 \pm 0.004$	$8.367 \pm 0.001$	$0.267 \pm 0.004$	$2.681 \pm 0.017$
C91H <sub>3</sub>	$4.035 \pm 0.004$	$3.929 \pm 0.001$	$0.106 \pm 0.004$	$2.689 \pm 0.019$

[a] The individual results  $\text{p}K_{\text{a}}^*$  of the different evaluated protons for the deprotonation of  $\text{N1aH}^+$  are given with one standard deviation ( $1\sigma$ ). The chemical shifts were calculated by using the final  $\text{p}K_{\text{a,H}_2\text{O}}$  value. The error ranges given with the calculated shifts are twice the standard deviation ( $2\sigma$ ). The shift differences  $\Delta\delta$ , resulting from the increasing deprotonation of the species are also listed:  $\Delta\delta_1 = \delta_{\text{NbH}} - \delta_{\text{Nb}}$ .

From these, the weighted mean was calculated to give  $\text{p}K_{\text{a,D}_2\text{O}} = 2.69 \pm 0.02$  ( $3\sigma$ ). This value was transformed to aqueous solution<sup>[30]</sup> to give the final result of  $\text{p}K_{\text{a,H}_2\text{O}} = 2.21 \pm 0.02$ . The error corresponds to three times the standard deviation. The calculated shifts of the protonated/deprotonated forms of **1c** are listed in Table 4.

As the adenine N1 position is platinated in both triplets **4a** and **4b**, no acid–base equilibria can be observed for this position. However, two deprotonation processes are expected in the pH range from 0 to 14: deprotonation of the guanine N1 position at  $\text{pH} \approx 8$  and deprotonation of the N6H<sub>2</sub> group of the adenine ligand in more alkaline medium. Changes in chemical shifts of all CH protons in the complexes due to the change in pD were evaluated as mentioned above using an equation which takes both equilibria into account.<sup>[28, 29]</sup> The determination of the acidity constants of complex **4a** has been described<sup>[28]</sup> and **4b** was treated accordingly. The chemical shifts of all non-exchangeable protons of the adenine and the guanine moieties could be evaluated, although H8 of 9-EtA disappeared at pD values greater than 12.2 due to isotopic exchange for deuterium atoms from the solvent, resulting in a smaller pD range for calculating the  $\text{p}K_{\text{a}}$  values than for the other protons. As examples, the chemical shifts of H2 of 9-EtA and H8 of the guanine ligand in **4b** are displayed in Figure 8b. The calculated individual acidity constants ( $\text{p}K_{\text{a}}^*$ ) for each proton are listed in Table 5. The corresponding chemical shifts of all protons evaluated in **4b** are listed in Table 6.

Table 5. Calculated negative logarithms of the individual acidity constants  $\text{p}K_{\text{a,G}}^*$  (for the deprotonation of N1gH) and  $\text{p}K_{\text{a,A}}^*$  (for the deprotonation of N6aH<sub>2</sub>) for the complex **4b** as determined in  $\text{D}_2\text{O}$  ( $20^\circ\text{C}$ ,  $I=0.1\text{ M}$ ,  $\text{NaNO}_3$ , see also Figure 8). All errors correspond to one standard deviation ( $1\sigma$ ).

	$\text{p}K_{\text{a,G}}^*$	$\text{p}K_{\text{a,A}}^*$
A–H2	$8.64 \pm 0.59$	$12.63 \pm 0.013$
A–H8	$8.45 \pm 0.27$	$12.65 \pm 0.017$
A–C91H <sub>2</sub>	$8.87 \pm 0.25$	$12.61 \pm 0.015$
A–C92H <sub>3</sub>	$9.36 \pm 0.59$	$12.63 \pm 0.018$
G–H8	$8.61 \pm 0.02$	$12.70 \pm 0.358$
G–C91H <sub>2</sub>	$8.59 \pm 0.03$	$12.52 \pm 0.042$
G–C92H <sub>3</sub>	$8.70 \pm 0.05$	$12.68 \pm 0.105$



Table 6. Chemical shifts of the protons for the undeprotonated, monodeprotonated, and twofold deprotonated forms of **4b** as determined in D<sub>2</sub>O (20 °C; *I* = 0.1 M, NaNO<sub>3</sub>, see also Figure 8).<sup>[a]</sup>

	$\delta_{\text{Nbh}_2}$	$\delta_{\text{Nbh}}$	$\delta_{\text{Nb}}$	$\Delta\delta_1$	$\Delta\delta_2$
ppm					
A-H2	9.007 ± 0.002	8.997 ± 0.002	8.431 ± 0.004	0.010 ± 0.003	0.566 ± 0.004
A-H8	8.917 ± 0.001	8.903 ± 0.001	8.418 ± 0.007	0.014 ± 0.001	0.485 ± 0.007
A-C91H <sub>2</sub>	4.448 ± 0.001	4.439 ± 0.001	4.239 ± 0.002	0.009 ± 0.001	0.200 ± 0.003
A-C92H <sub>3</sub>	1.562 ± 0.001	1.560 ± 0.001	1.481 ± 0.001	0.002 ± 0.001	0.079 ± 0.001
G-H8	8.569 ± 0.001	8.373 ± 0.001	8.386 ± 0.002	0.196 ± 0.001	-0.013 ± 0.003
G-C91H <sub>2</sub>	4.247 ± 0.001	4.210 ± 0.001	4.181 ± 0.001	0.037 ± 0.001	0.029 ± 0.001
G-C92H <sub>3</sub>	1.511 ± 0.001	1.496 ± 0.001	1.480 ± 0.002	0.015 ± 0.001	0.016 ± 0.003

[a] The chemical shifts were calculated by using the final  $pK_{\text{a,D}_2\text{O}}$  values. The error limits given correspond to two times the standard deviation ( $2\sigma$ ). The shift differences  $\Delta\delta$ , resulting from the increasing deprotonation of the species are also listed:  $\Delta\delta_1 = \delta_{\text{Nbh}_2} - \delta_{\text{Nbh}}$ ;  $\Delta\delta_2 = \delta_{\text{Nbh}} - \delta_{\text{Nb}}$ .

From the  $pK_{\text{a}}^*$  values the weighted means were taken to give the acidity constants valid for D<sub>2</sub>O solution ( $pK_{\text{a,G/D}_2\text{O}} = 8.61 \pm 0.08$  ( $3\sigma$ ),  $pK_{\text{a,A/D}_2\text{O}} = 12.62 \pm 0.03$  ( $3\sigma$ )). These values were then transformed to the  $pK_{\text{a}}$  values valid for water:<sup>[30]</sup>  $pK_{\text{a,G/H}_2\text{O}} = 8.04 \pm 0.08$  ( $3\sigma$ ),  $pK_{\text{a,A/H}_2\text{O}} = 11.99 \pm 0.03$  ( $3\sigma$ ). Both values are very similar to those of complex **4a**:  $pK_{\text{a,G/H}_2\text{O}} = 8.33 \pm 0.09$  ( $3\sigma$ ) and  $pK_{\text{a,A/H}_2\text{O}} = 12.06 \pm 0.10$  ( $3\sigma$ ).<sup>[28]</sup>

With respect to the monoplatinated guanine moieties the acidification of the N1H position by the N7-coordinated Pt<sup>II</sup> unit can be determined by comparing the results obtained with the  $pK_{\text{a}}$  value of free 9-EtGH ( $pK_{\text{a}} = 9.54 \pm 0.08$ ).<sup>[28]</sup>

$$\text{for } \mathbf{4a}: \Delta pK_{\text{a}} = (9.54 \pm 0.08) - (8.33 \pm 0.09) = 1.21 \pm 0.12$$

$$\text{for } \mathbf{4b}: \Delta pK_{\text{a}} = (9.54 \pm 0.08) - (8.04 \pm 0.08) = 1.50 \pm 0.11$$

Both  $\Delta pK_{\text{a}}$  values are close to data found in the literature for other platinated guanine compounds.<sup>[31]</sup>

The values for the deprotonation of the exocyclic N6H<sub>2</sub> groups of the adenine ligands are identical within their error limits in both complexes. Compared with the value for free 9-MeA ( $pK_{\text{a}} = 16.7$ ).<sup>[32]</sup> the acidification is very pronounced and amounts to  $\Delta pK_{\text{a}} = 16.7 - 12.0$  (av of **4a** and **4b**) = 4.7. This result is not surprising, since the adenine nucleobase is bound to two Pt<sup>2+</sup> centers that have electron-withdrawing effects.

**Platinated nucleobase sextet:** Recrystallization of **5** from water with an excess of perchlorate gave crystals suitable for X-ray crystallography. The asymmetric unit contains one formula unit of the diplatinated nucleobase triplet *trans,trans*-(NH<sub>3</sub>)<sub>2</sub>Pt(1-MeU-N3)( $\mu$ -9-EtA-N7,N1)Pt(NH<sub>2</sub>CH<sub>3</sub>)<sub>2</sub>(9-EtGH<sub>0.5</sub>-N7)](ClO<sub>4</sub>)<sub>2.5</sub> · 1.25 H<sub>2</sub>O; upon dimerization a nucleobase sextet is formed containing a homoguanine/guaninate basepair as shown in Figure 9. The atoms of the half-occupied perchlorate molecule are found on general positions and the 1.25 water molecules are distributed over three positions with occupancy factors of 50, 50, and 25%. For further details regarding structure and refinement see Table 1 and for some selected bond lengths and angles as well as their comparison with complexes **2a** and **4a** see Table 3.

As observed in the complexes described above, also in this structure a mixture of two rotamers concerning the orienta-

tion of the uracil ligand is found (65:35). The rotamer with N1'-CH<sub>3</sub> pointing outwards is the dominant one. Due to the two intramolecular hydrogen bonds present in each nucleobase triplet (O4'...N6a, 3.35(3) Å; N6a...O6g, 3.17(2) Å) the platinum coordination spheres are distorted square planar with angles N7a-Pt1-N3' and N1a-Pt2-N7g of 176.6(9)° and 176.9(9)° (see also Table 3).

In addition to these four intramolecular hydrogen

bonds holding the two triplets together are found. Three are between the two 9-ethylguanine bases. Two of these are between O6g and N2g (2.78(4) Å) and one is between the N1g...N1g atoms (2.90(5) Å). Each amino group of the 9-EtGH<sub>0.5</sub> ligands undergoes additional hydrogen bonding

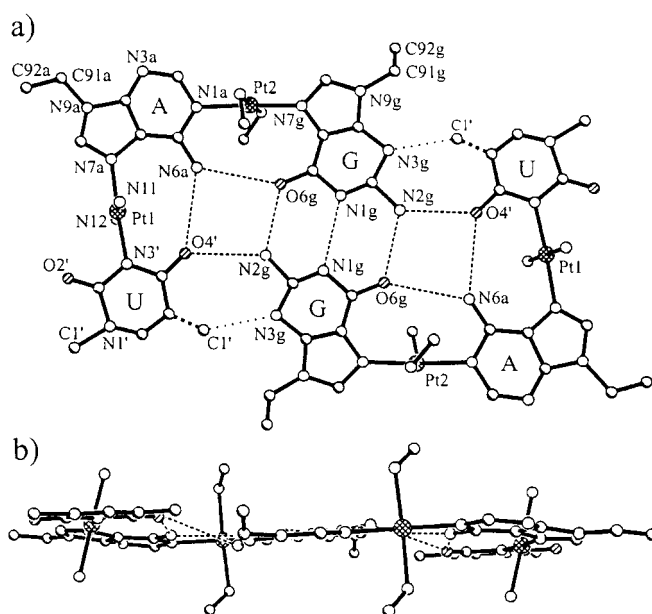


Figure 9. Top (a) and side (b) view of two diplatinated nucleobase triplets, which are hemideprotonated at the guanine N1 position forming the tetraplatinated nucleobase sextet **5** with the atomic numbering scheme. Hydrogen bonds are indicated by dashed, and longer contacts by dotted lines. The water molecules and the anions are omitted for clarity.

(3.01(4) Å) with the nearby exocyclic carbonyl oxygen atoms of the uracil bases (O4' or O2', respectively), thereby reinforcing the linkage between the two cations. A further contact between the two triplets is formed between N3g and C1'H3 of the minor rotamer (2.9(1) Å).

Contacts between two sextets are formed through two hydrogen bonds around an inversion center involving the amine ligands and N3a of the adenine moieties (3.12(2) Å, Figure 10). In this way infinite chains of sextets are formed within the crystal.

The sextet is almost planar, as depicted in Figure 9b. The two 9-EtGH<sub>0.5</sub> nucleobases are coplanar and the angles between the 9-EtGH<sub>0.5</sub>/9-EtA and 9-EtA/1-MeU nucleobases are 10.4(6)° and 7.6(9)°, respectively. The 9-EtGH<sub>0.5</sub> and the 1-MeU ligands are almost parallel (3(1)°), even though they are not coplanar.

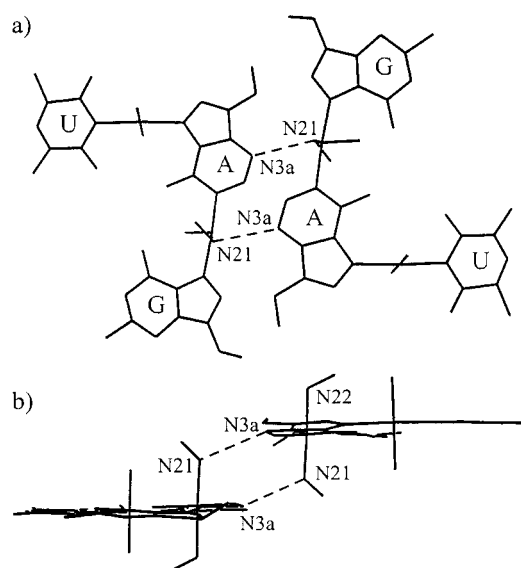


Figure 10. Dimerization of cations of **5** around an inversion center through two hydrogen bonds between amine ligands and N3 of the adenine moieties. Views from the top (a) and from the side (b).

Two related sextet structures have been published recently,<sup>[33]</sup> both consist of a diplatinated 9-methyladenine moiety and two 9-methylguanine or 9-methylhypoxanthine ligands, respectively. Dimerization of two triplets is in both cases accomplished through two hydrogen bonds between two hypoxanthine or guanine moieties as well as base stacking. Since the guanines are not deprotonated, the sextets are not planar.

The same triplet which leads to **5** also gives rise to a nucleobase quartet upon hydrogen bonding formation with 1-methylcytosine in the solid state as well as in solution.<sup>[17a, 28]</sup>

**Solution studies of 5:** NOESY experiments in [D<sub>7</sub>]DMF have been carried out in order to prove the sextet formation in solution. Indeed a NOE is found between H6' of the uracil and the ethyl groups of the guanine ligands (data not shown) which clearly indicates the dimerization.

It was also attempted to determine the association constant of the dimerization of the two hemideprotonated triplets to give **5** through concentration-dependent chemical shift measurements in [D<sub>6</sub>]DMSO in analogy to the procedure described in the literature,<sup>[18b]</sup> where the dimerization of *trans*-[(NH<sub>3</sub>)<sub>2</sub>Pt(1-MeC-N3)(9-EtG-N7)]<sup>+</sup> has been examined. Unfortunately the obtained data set allowed only a rough estimation of the association constant, as the N1gH resonance was too broad to be detected and evaluated, and the resonances of N2gH<sub>2</sub> of 9-EtGH<sub>0.5</sub> and H6' of the uracil ligand are superimposed. Nevertheless, both resonances display concentration-dependent chemical shifts. Surprisingly,

the resonance of one of the protons of the adenine N6aH<sub>2</sub> group showed the most pronounced dependence in concentration as can be seen from Figure 11, though this proton is

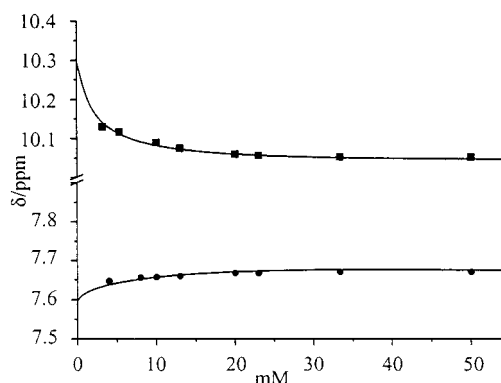


Figure 11. Concentration dependence of the chemical shifts of **5** in [D<sub>6</sub>]DMSO in the concentration range 0–55 mM. The data from top to bottom correspond to one proton of N6H<sub>2</sub> (■) and the resonances of N2H<sub>2</sub> of 9-EtGH<sub>0.5</sub> and H6' of 1-MeU (●) which are superimposed. The curve corresponds to the fit<sup>[28]</sup> of the data with the estimated  $K_D = 500 \text{ M}^{-1}$  ( $\delta_0 = 10.305$  and  $7.586$ ;  $\delta_D = 10.006$  and  $7.685$ ).

not directly involved in the intermolecular hydrogen bonding. Furthermore, this proton is shifted *upfield* with increasing concentrations, thus showing exactly the opposite behavior one normally observes with the intermolecular association of molecules through hydrogen bonding.<sup>[28]</sup> However, this finding can be rationalized in the following way: Upon dimerization of hemideprotonated **4b** to the sextet **5**, O6g of the 9-EtGH<sub>0.5</sub> ligand will be increasingly involved in intermolecular hydrogen bonding with N2gH<sub>2</sub> of the opposite guanine moiety. Consequently, the intramolecular hydrogen bond to N6aH<sub>2</sub><sup>1</sup> of 9-EtA is weakened and this proton should then experience an upfield shift as is experimentally confirmed. Comparison of H bond lengths between N6aH<sub>2</sub> and O6g in the solid state indeed reveals that hemideprotonation of guanine leads to a significant increase, from 3.019(9) Å in **4b** to 3.17(2) Å in **5** (Table 3). The second proton, N6aH<sub>2</sub><sup>2</sup>, is almost unaffected by the change in concentration, thus it can be concluded that it points towards the O2'/O4' carbonyl oxygen of 1-MeU, as: 1) this hydrogen bond has been shown to be nonexistent in the precursor compounds in [D<sub>6</sub>]DMSO solution (see above) and 2) in the crystal structure of **5**, this distance is even longer (3.35(3) Å) than in the precursor complexes (see Table 2 and Table 3). This concentration-dependent splitting of the resonances of N6aH<sub>2</sub> closely resembles that of N4H<sub>2</sub> of the 1-MeC ligand in the dimerization of *trans*-[(NH<sub>3</sub>)<sub>2</sub>Pt(1-MeC-N3)(9-EtG-N7)]<sup>+</sup>.<sup>[18]</sup>

Evaluation of the chemical shifts of N2gH<sub>2</sub> and N6aH<sub>2</sub> did not lead to unequivocal results, that is the values obtained for  $K_D$  carried a very large error, as the shift differences are small due to the high stability of **5**. This means that the formation degree of **5** is large under the given experimental conditions (low concentrations). Hence, it was decided to vary  $K_D$  systematically in the range of 200 to 800 M<sup>-1</sup> and to see which of the values fitted the experimental data points in a reasonable way. It turned out that a very satisfactory fit of

both data series is obtained with  $K_D = 500 \text{ M}^{-1}$  (Figure 11). Fits with values of 350 and  $650 \text{ M}^{-1}$  were considerably less satisfactory. Hence, the association constant  $K_D$  of dimer **5** was estimated to be  $K_D = 500 \pm 150 \text{ M}^{-1}$ .

However, despite the fact that only a rough estimate for  $K_D$  could be obtained, it is clear that dimerization of hemideprotonated **4b** through five intermolecular hydrogen bonds gives rise to a rather stable dimeric adduct in  $[\text{D}_6]\text{DMSO}$ . Indeed, comparison of  $K_D = 500 \pm 150 \text{ M}^{-1}$  with the value determined for the dimerization of *trans*- $[(\text{NH}_3)_2\text{Pt}(1\text{-MeC-N3})(9\text{-EtG-N7})]^+$  ( $K_D = 44.1 \pm 3.2 \text{ M}^{-1}$  ( $2\sigma$ )), which is stabilized through four hydrogen bonds, and with those for the association of several platinated and non-platinated guanine derivatives with 1-MeC in a Watson–Crick type fashion through three hydrogen bonds in the same solvent ( $K_{\text{GC}}$  between  $6.9 \pm 1.3 \text{ M}^{-1}$  and  $22 \pm 10 \text{ M}^{-1}$  ( $2\sigma$ )),<sup>[28]</sup> demonstrates nicely the interrelation between the stability of the adducts and the number of hydrogen bonds involved in their formation.

Finally, the fact that only the hemideprotonated sextet **5** and not the triplet **4b** could be isolated from aqueous solution even at pH 4 (i.e., a pH where N1 of 9-EtGH is expected to be fully protonated) shows, that this entity is exceedingly stable.

## Conclusion

Higher order architecture beyond duplex formation is an emerging feature of nucleic acid chemistry.<sup>[34]</sup> Thus in addition to the well-known guanine quartets ( $G_4$ ) present in telomeric DNA sequences,<sup>[35]</sup> numerous other multistranded nucleic acid structures with nucleobase triplets,<sup>[36]</sup> quartets,<sup>[37]</sup> and sextets<sup>[38]</sup> have been discovered in recent years. In a number of cases the pivotal role of alkali metal ions in stabilizing such structures has been clearly established.<sup>[39]</sup> The nature of the alkali metal ion may even influence the way base pairs interact, thus behaving as a conformational switch.<sup>[40]</sup> Moreover, the specific folding of DNA aptamers in the presence of  $\text{K}^+$  is believed to generate defined architectures responsible for inhibition of crucial HIV enzymes.<sup>[41]</sup>

Transition metal ions with their ability for coordinative bond formation and hence crosslinking of nucleobases are likewise expected to produce ordered multistranded oligonucleotide structures, although this phenomenon has been studied in the case of  $\text{Ag}^+$  ions only.<sup>[2e]</sup> Our studies with complexes of model nucleobases and linear *trans*-diam(m)ine-platinum(II) entities strongly suggest that, in principle, any metal ion with a linear coordination geometry might be capable of producing regular multistranded structures. In addition, if nucleobase deprotonation occurs, as reported for oligonucleotides in the presence of  $\text{Ag}^I$  and  $\text{Hg}^{II}$ , for example,<sup>[1,2]</sup> rather robust aggregates are expected to be formed. Moreover, it is expected that interbase H bond formation will be influenced. Here we have synthesized and characterized a number of complexes, consisting of an adenine and a pyrimidine ligand each, crosslinked by a linear *trans*- $\text{a}_2\text{Pt}^{II}$  moiety, which were potential candidates for dimerization and thus quartet formation. Subsequent addition of a *trans*- $\text{a}_2\text{Pt}^{II}$  entity and guanine ligand as a third

nucleobase led to two different triplet structures, which were again studied by X-ray crystallography and whose  $\text{p}K_a$  values were determined by NMR spectroscopy. We have demonstrated that one of these nucleobase triplets associates through a hemideprotonated guanine pair to form an extremely stable platinated sextet, which by far exceeds all known nucleobase H bonding patterns in strength.

## Experimental Section

**Materials:** *trans*- $[(\text{NH}_3)_2\text{PtCl}_2]$ <sup>[42]</sup> and *trans*- $[(\text{CH}_3\text{NH}_2)_2\text{PtCl}_2]$ <sup>[43]</sup> were synthesized from  $\text{K}_2\text{PtCl}_4$  (Hereaus, Hanau (Germany)) according to the literature. 9-Ethylguanine was purchased from Chemogen, Konstanz (Germany). 1-Methylthymine,<sup>[44]</sup> 1-methyluracil,<sup>[45]</sup> 9-ethyladenine,<sup>[46]</sup> 9-methyladenine,<sup>[47]</sup> and 1-methylcytosine<sup>[48]</sup> were prepared as described. Compounds **1b–d** have been synthesized in analogy to **1a**, as described in reference [11]. The synthesis of **2b** has already been described<sup>[17a]</sup> and **2a** was prepared analogously. The preparation of **5** is likewise reported in reference [17a]. All other chemicals used (either *puriss* or *pro analysi*) were from Merck GmbH, Darmstadt (Germany), Fluka AG, Buchs (Switzerland) or Aldrich-Chemical Co. Ltd., Gillingham-Dorset (UK).

*trans,trans*- $[(\text{NH}_3)_2\text{Pt}(1\text{-MeT-N3})(\mu\text{-9-MeA-N7,N1})\text{Pt}(\text{NH}_2\text{CH}_2)_2(\text{DMSO})]^{3+}$  (**3a**) and *trans,trans*- $[(\text{NH}_3)_2\text{Pt}(1\text{-MeU-N3})(\mu\text{-9-EtA-N7,N1})\text{Pt}(\text{NH}_2\text{CH}_2)_2(\text{DMSO})]^{3+}$  (**3b**): Complex **2a** or **2b**, respectively (11 mg, 10.5  $\mu\text{mol}$ ; 16 mg, 15.9  $\mu\text{mol}$ ) were dissolved in  $[\text{D}_6]\text{DMSO}$  (400  $\mu\text{L}$ ), and <sup>195</sup>Pt NMR spectra were recorded immediately. Additional spectra were taken after 30, 40, 60, 70, 80, 100, 120 min, and one more after 12 h when the substitution reaction of the chloro ligand by a solvent molecule was completed. Compounds **3a** and **3b** were not isolated.

**3a:** <sup>1</sup>H NMR (200 MHz,  $[\text{D}_6]\text{DMSO}$ ):  $\delta = 9.7$  (s;  $\text{H}_2\text{N6a}$ ), 8.620 (s;  $\text{H8a}$ ), 8.319 (s;  $\text{H2a}$ ), 7.326/7.319 (s, rotamers;  $\text{H6}'$ ), 4.9 (m;  $\text{H}_2\text{N20}$ ,  $\text{H}_2\text{N21}$ ), 3.930 (s;  $\text{H}_3\text{N10}$ ,  $\text{H}_3\text{N11}$ ), 3.842 (s;  $\text{H}_3\text{C9a}$ ), 3.228 (s;  $\text{H}_3\text{C1}'$ ), 2.334 (t,  $^3J = 6$  Hz;  $\text{H}_3\text{C20}$ ,  $\text{H}_3\text{C21}$ ), 1.765/1.760 (s, rotamers;  $\text{H}_3\text{C51}'$ ); <sup>195</sup>Pt NMR (42.998 MHz,  $[\text{D}_6]\text{DMSO}$ ):  $\delta = -2470$ ,  $-3169$ .

**3b:** <sup>1</sup>H NMR (200 MHz,  $[\text{D}_6]\text{DMSO}$ ):  $\delta = 9.9$  (s;  $\text{H}_2\text{N6a}$ ), 8.680 (s;  $\text{H8a}$ ), 8.315 (s;  $\text{H2a}$ ), 7.410 (d,  $^3J = 6$  Hz;  $\text{H6}'$ ), 5.408 (d,  $^3J = 6$  Hz;  $\text{H5}'$ ), 4.9 (m;  $\text{H}_2\text{N20}$ ,  $\text{H}_2\text{N21}$ ), 4.298 (q,  $^3J = 7$  Hz;  $\text{H}_2\text{C91a}$ ), 3.9 (s;  $\text{H}_3\text{N10}$ ,  $\text{H}_3\text{N11}$ ), 3.266 (s;  $\text{H}_3\text{C1}'$ ), 2.364 (t,  $^3J = 6$  Hz;  $\text{H}_3\text{C20}$ ,  $\text{H}_3\text{C21}$ ), 1.469 (t,  $^3J = 7$  Hz;  $\text{H}_3\text{C92a}$ ); <sup>195</sup>Pt NMR (42.998 MHz,  $[\text{D}_6]\text{DMSO}$ ):  $\delta = -2465$ ,  $-3173$ .

*trans,trans*- $[(\text{NH}_3)_2\text{Pt}(1\text{-MeT-N3})(\mu\text{-9-MeA-N7,N1})\text{Pt}(\text{NH}_2\text{CH}_2)_2(9\text{-EtGH-N7})](\text{ClO}_4)_3$  (**4a**): Compound **2a** (400 mg, 383  $\mu\text{mol}$ ) and  $\text{AgNO}_3$  (62 mg, 0.95 equiv) were stirred at 40 °C in the dark overnight in  $\text{H}_2\text{O}$  (50 mL). After removal of  $\text{AgCl}$ , 9-EtGH (83 mg, 1.2 equiv) was added, the solution adjusted to pH 4.0 ( $\text{HNO}_3$ ) and stirred at 40 °C for two days. The solution was readjusted to pH 7 ( $\text{NaOH}$ ) and slowly concentrated at room temperature under a steady flux of  $\text{N}_2$  during which excess of 9-EtGH was removed by filtration. The residue remaining after evaporation was recrystallized from water to give **4a** (187 mg; 39% yield).

**4a:** <sup>1</sup>H NMR (200 MHz,  $\text{D}_2\text{O}$ ):  $\delta = 9.020$  (s;  $\text{H2a}$ ), 8.850 (s;  $\text{H8a}$ ), 8.556 (s;  $\text{H8g}$ ), 7.385 (s;  $\text{H6}'$ ), 4.244 (q,  $^3J = 7$  Hz;  $\text{H}_2\text{C91g}$ ), 4.005 (s;  $\text{H}_3\text{C9a}$ ), 3.465/3.953 (s, rotamers;  $\text{H}_3\text{C1}'$ ), 2.123 (s;  $\text{H}_3\text{C20}$ ,  $\text{H}_3\text{C21}$ ), 1.961/1.895 (s, rotamers;  $\text{H}_3\text{C51}'$ ), 1.510 (t,  $^3J(\text{H,H}) = 7$  Hz;  $\text{H}_3\text{C92g}$ ); <sup>1</sup>H NMR (200 MHz,  $[\text{D}_6]\text{DMSO}$ ):  $\delta = 11.9$  (s,  $\text{H1g}$ ), 10.30/10.07 ( $\text{H}_2\text{N6a}$ ), 8.887 (s;  $\text{H8a}$ ), 8.825 (s;  $\text{H2a}$ ), 8.410 (s;  $\text{H8g}$ ), 7.4 ( $\text{H}_2\text{N2g}$ ), 7.391 (s;  $\text{H6}'$ ), 5.0 (m;  $\text{H}_2\text{N20}$ ,  $\text{H}_2\text{N21}$ ), 4.126 (q,  $^3J = 7$  Hz;  $\text{H}_2\text{C91g}$ ), 3.97–4.08 ( $\text{H}_3\text{N10}$ ,  $\text{H}_3\text{N11}$ ,  $\text{H}_3\text{C9a}$ ,  $\text{H}_3\text{C1}'$ ), 3.348 (s;  $\text{H}_3\text{C1}'$ ), 1.446 (t,  $^3J = 7$  Hz;  $\text{H}_3\text{C92g}$ ); <sup>195</sup>Pt NMR (42.998 MHz,  $\text{D}_2\text{O}$ ):  $\delta = -2500$ ,  $-2621$ ; FT-IR (KBr):  $\tilde{\nu} = 3291$ , 3147, 1686, 1635, 1592, 1561, 1440, 1367, 1230, 1090, 781, 719, 684, 625, 463, 280  $\text{cm}^{-1}$ ; elemental analysis calcd (%) for  $\text{C}_{21}\text{H}_{39}\text{N}_{16}\text{O}_{15}\text{Cl}_3\text{Pt}_2$  (1252.16): C 20.14; H 3.14; N 17.90; found: C 20.2; H 3.2; N 18.1 (anhydrous complex). According to X-ray analysis, 5.2 water molecules are present in freshly prepared crystals of **4a**.

**Determination of acidity constants:** The  $\text{p}K_a$  values of complexes **1c**, **4a**, and **4b** were determined using pH-dependent <sup>1</sup>H NMR spectroscopic measurements in  $\text{D}_2\text{O}$  (20 °C;  $I = 0.1 \text{ M}$ ,  $\text{NaNO}_3$ ). Changes in chemical shifts of all non-exchangeable protons in the complexes due to the change in pD were evaluated with a nonlinear least-squares fit after Newton–Gauss.<sup>[28, 29]</sup>

The obtained acidity constants were then transformed to the values valid for water according to the literature.<sup>[30]</sup>

**Determination of stability constants:** Determination of the association constant  $K_D$  of the dimerization of the two hemideprotonated triplets of **4b** to give **5** was performed by using concentration-dependent chemical shift measurements in  $[D_6]DMSO$  in analogy to the procedure described in the literature.<sup>[18b]</sup>

**Crystal structure analysis:** Intensity data of **1b** was collected on a Siemens P4 four-circle diffractometer with graphite-monochromated  $MoK_{\alpha}$  radiation ( $\lambda = 0.71069 \text{ \AA}$ ) using the  $\omega$  scan technique with variable scan speed ( $3\text{--}15^\circ \text{ min}^{-1}$ ). Three standard reflections measured every 100 data points showed no systematic variation in intensity. The data have been corrected for absorption, Lorentz, and polarization effects using the data reduction program XDISK.<sup>[49]</sup> An empirical absorption correction was carried out using azimuth ( $\psi$ ) scans. For the data collection of **1c**, **1d**, **2a**, **4a**, and **5**, an Enraf–Nonius KappaCCD<sup>[50]</sup> ( $MoK_{\alpha}$ ,  $\lambda = 0.71069 \text{ \AA}$ , graphite-monochromator) was used. Sample-to-detector distances were 26.7 (**2a**), 28.7 (**1c**), 30.2 (**4a**), 30.7 (**1d**), and 32.2 (**5**), respectively. The whole sphere of reciprocal space was covered by measurement of 360 frames rotating about  $\omega$  in steps of  $1^\circ$ . The exposure times were 10 (**2a**), 60 (**1d**, **4a**), 75 (**1c**), and 100 s (**5**) per frame. Preliminary orientation matrices and unit cell parameters were obtained from the peaks of the first ten frames, respectively, and refined by using the whole data set. Frames were integrated and corrected for Lorentz and polarization effects using DENZO.<sup>[51]</sup> The scaling as well as the global refinement of crystal parameters were performed by SCALEPACK.<sup>[51]</sup> Reflections, which were partly measured on previous and following frames, are used to scale these frames on each other. Merging of redundant reflections in part eliminates absorption effects and also considers crystal decay if present.

The structures were solved by standard Patterson methods<sup>[52]</sup> and refined by full-matrix least-squares based on  $F^2$  using the SHELXTL-PLUS<sup>[49]</sup> and SHELXL-93 programs.<sup>[53]</sup> The scattering factors for the atoms were those given in the SHELXTL-PLUS program. Transmission factors were calculated with SHELXL-97.<sup>[54]</sup> Hydrogen atoms were included in calculated positions and refined with isotropic displacement parameters according to the riding model, except for H8 in **1b**, which could be localized with difference-Fourier synthesis. Displacement factors for the protons in structures **1c** (except the methyl and ammine protons) and **5** were assigned according to  $U(H) = 1.3 U(C_{\text{bonded}}/N_{\text{bonded}})$  in order to save parameters because of the poor observed reflection to parameter ratios. For the same reason a part of the ring atoms in **1c** and **1d** as well as all non-hydrogens atoms except for the two Pt atoms in **5** were only refined isotropically.

Crystallographic data (excluding structure factors) for the structures reported in this paper have been deposited with the Cambridge Crystallographic Data Centre as supplementary publication nos. CCDC-150799 (**1b**), CCDC-150800 (**1c**), CCDC-150801 (**1d**), CCDC-150802 (**2a**), CCDC-150803 (**4a**), and CCDC-150804 (**5**). Copies of the data can be obtained free of charge on application to CCDC, 12 Union Road, Cambridge CB2 1EZ, UK (fax: (+44)1223-336-033; e-mail: deposit@ccdc.cam.ac.uk).

## Acknowledgement

This work has been supported by the Deutsche Forschungsgemeinschaft (DFG) and the Fonds der Chemischen Industrie (FCI).

- [1] a) S. Katz, *J. Am. Chem. Soc.* **1952**, *74*, 2238; b) C. A. Thomas, *J. Am. Chem. Soc.* **1954**, *76*, 6032; c) T. Yamane, N. Davidson, *J. Am. Chem. Soc.* **1961**, *83*, 2599; d) G. L. Eichhorn, P. Clark, *J. Am. Chem. Soc.* **1963**, *85*, 4020; e) R. B. Simpson, *J. Am. Chem. Soc.* **1964**, *86*, 2059.
- [2] a) T. Yamane, N. Davidson, *Biochim. Biophys. Acta* **1962**, *55*, 609; b) R. H. Jensen, N. Davidson, *Biopolymers* **1966**, *4*, 17; c) M. Daune, C. A. Dekker, H. K. Schachman, *Biopolymers* **1966**, *4*, 51; d) G. L. Eichhorn, J. J. Butzow, P. Clark, E. Tarien, *Biopolymers* **1967**, *5*, 283; e) Y. A. Shin, G. L. Eichhorn, *Biopolymers* **1980**, *19*, 539.
- [3] a) M. Sundaralingam, J. A. Carrabine, *J. Mol. Biol.* **1971**, *61*, 287; b) E. Sletten in *Metal-Ligand Interactions in Organic Chemistry and Biochemistry* (Eds.: B. Pullman, N. Goldblum), Riedel, Dordrecht, **1977**, p. 33.
- [4] For  $Hg^{II}$ : a) L. D. Kosturko, C. Folzer, R. F. Stewart, *Biochemistry* **1974**, *13*, 3949; b) B. J. Graves, D. J. Hodgson, *Inorg. Chem.* **1981**, *20*, 2223; c) F. Zamora, M. Sabat, B. Lippert, *Inorg. Chim. Acta* **1998**, *267*, 87. The list does not include examples of  $HgCl_2$  adducts of nucleobases nor examples of nucleobase complexes of organomercurials such as  $CH_3Hg^{II}$ , for example.
- [5] For  $Ag^I$ : a) C. Gagnon, A. L. Beauchamp, *Inorg. Chim. Acta* **1975**, *14*, L52; b) L. G. Marzilli, T. J. Kistenmacher, M. Rossi, *J. Am. Chem. Soc.* **1977**, *99*, 2797; c) T. J. Kistenmacher, M. Rossi, L. G. Marzilli, *Inorg. Chim. Acta* **1979**, *18*, 240; d) F. Guay, A. L. Beauchamp, *J. Am. Chem. Soc.* **1979**, *101*, 6260; e) F. Bélanger-Gariépy, A. L. Beauchamp, *J. Am. Chem. Soc.* **1980**, *102*, 3461; f) K. Aoki, W. Saenger, *Acta Crystallogr.* **1984**, *C40*, 775; g) S. Menzer, M. Sabat, B. Lippert, *J. Am. Chem. Soc.* **1992**, *114*, 4644; h) S. Menzer, E. C. Hillgeris, B. Lippert, *Inorg. Chim. Acta* **1993**, *210*, 167.
- [6] For  $Cu^{II}$  see for example: D. Tran Qui, E. Palacios, *Acta Crystallogr. Sect. C* **1990**, *46*, 1220.
- [7] For  $Hg^{II}$ , see for example: N. A. Froystein, E. Sletten, *J. Am. Chem. Soc.* **1994**, *116*, 3240 and references therein.
- [8] For a recent update on this topic, see: *Cisplatin-Chemistry and Biochemistry of a Leading Anticancer Drug* (Ed.: B. Lippert), HVCA, Zürich, and Wiley-VCH, Weinheim, **1999**.
- [9] See, for example: a) V. Brabec, M. Leng, *Proc. Natl. Acad. Sci. USA* **1993**, *90*, 5345; b) V. Brabec, M. Sip, M. Leng, *Biochemistry* **1993**, *32*, 11676; c) B. Andersen, E. Bernal-Méndez, M. Leng, E. Sletten, *Eur. J. Inorg. Chem.* **2000**, 1201.
- [10] a) B. Lippert in *Met. Ions Biol. Syst. Vol. 33* (Eds.: A. Sigel, H. Sigel), Marcel Dekker, Inc., New York, Basel, Hong Kong, **1996**, p. 105; b) E. Zangrando, F. Pichierri, L. Randaccio, B. Lippert, *Coord. Chem. Rev.* **1996**, *156*, 275.
- [11] O. Krizanovic, M. Sabat, R. Beyerle-Pfnür, B. Lippert, *J. Am. Chem. Soc.* **1993**, *115*, 5538.
- [12] a) M. S. Lüth, E. Freisinger, F. Glahé, B. Lippert, *Inorg. Chem.* **1998**, *37*, 5044; b) M. S. Lüth, E. Freisinger, F. Glahé, J. Müller, B. Lippert, *Inorg. Chem.* **1998**, *37*, 3195; c) A. Schreiber, M. S. Lüth, A. Erxleben, E. C. Fusch, B. Lippert, *J. Am. Chem. Soc.* **1996**, *118*, 4124.
- [13] A. Schreiber, E. C. Hillgeris, B. Lippert, *Z. Naturforsch. B* **1993**, *48*, 1603.
- [14] H. Rauter, I. Mutikainen, M. Blomberg, C. J. L. Lock, P. Amo-Ochoa, E. Freisinger, L. Randaccio, E. Zangrando, E. Chiarparin, B. Lippert, *Angew. Chem.* **1997**, *109*, 1353; *Angew. Chem. Int. Ed. Engl.* **1997**, *36*, 1296.
- [15] B. Lippert, *J. Chem. Soc. Dalton Trans.* **1997**, 3971.
- [16] C. Meiser, E. Freisinger, B. Lippert, *J. Chem. Soc. Dalton Trans.* **1998**, 2059.
- [17] a) R. K. O. Sigel, S. M. Thompson, E. Freisinger, B. Lippert, *Chem. Commun.* **1999**, 19; b) R. K. O. Sigel, E. Freisinger, B. Lippert, *Chem. Commun.* **1998**, 219.
- [18] a) S. Metzger, B. Lippert, *J. Am. Chem. Soc.* **1996**, *118*, 12467; b) R. K. O. Sigel, E. Freisinger, S. Metzger, B. Lippert, *J. Am. Chem. Soc.* **1998**, *120*, 12000.
- [19] M. S. Lüth, E. Freisinger, B. Lippert, unpublished results.
- [20] a) A. D. Burrows, C.-W. Chan, M. M. Chawdhry, J. E. McGrady, D. M. P. Mingos, *Chem. Soc. Rev.* **1995**, 329 and references therein; b) S. L. James, D. M. P. Mingos, X. Xu, A. J. P. White, D. J. Williams, *J. Chem. Soc. Dalton Trans.* **1998**, 1335; c) S. Ulvenlund, A. S. Georgopoulou, D. M. P. Mingos, I. Baxter, S. E. Lawrence, A. J. P. White, D. J. Williams, *J. Chem. Soc. Dalton Trans.* **1998**, 1869 and references therein; d) X. Xu, S. L. James, D. M. P. Mingos, A. J. P. White, D. J. Williams, *J. Chem. Soc. Dalton Trans.* **2000**.
- [21] I. Dieter-Wurm, M. Sabat, B. Lippert, *J. Am. Chem. Soc.* **1992**, *114*, 357.
- [22] W. L. Jorgensen, D. L. Severance, *J. Am. Chem. Soc.* **1991**, *113*, 209.
- [23] a) R. K. O. Sigel, M. Sabat, E. Freisinger, A. Mower, B. Lippert, *Inorg. Chem.* **1999**, *38*, 1481. b) F. Zamora, H. Witkowski, E. Freisinger, J. Mueller, B. Thormann, A. Albinati, B. Lippert, *J. Chem. Soc. Dalton Trans.* **1999**, 175.
- [24] D. Holthenrich, I. Sóvágó, G. Fusch, A. Erxleben, E. C. Fusch, I. Rombeck, B. Lippert, *Z. Naturforsch. B* **1996**, *50*, 1767.
- [25] M. N. Frey, T. F. Koetzle, M. S. Lehmann, W. C. Hamilton, *J. Chem. Phys.* **1973**, *59*, 915.

- [26] Y. Chen, Z. Guo, P. J. Sadler in *Cisplatin, Chemistry and Biochemistry of a Leading Anticancer Drug* (Ed.: B. Lippert), HVCA, Zürich, and Wiley-VCH, Weinheim, **1999**, p. 293.
- [27] a) T. G. Appleton, A. J. Bailey, K. J. Barnham, J. R. Hall, *Inorg. Chem.* **1992**, *31*, 3077; b) P. S. Pregosin, *Annu. Rep. NMR Spectrosc.* **1986**, *17*, 285.
- [28] a) R. K. O. Sigel, E. Freisinger, B. Lippert, *J. Biol. Inorg. Chem.* **2000**, *5*, 287; b) R. K. O. Sigel, B. Lippert, *Chem. Commun.* **1999**, 2167.
- [29] R. Tribolet, H. Sigel, *Eur. J. Biochem.* **1987**, *163*, 353.
- [30] R. B. Martin, *Science* **1963**, *139*, 1198.
- [31] a) B. Song, J. Zhao, R. Griesser, C. Meiser, H. Sigel, B. Lippert, *Chem. Eur. J.* **1999**, *5*, 2374; b) G. Schröder, B. Lippert, M. Sabat, C. J. L. Lock, R. Faggiani, B. Song, H. Sigel, *J. Chem. Soc. Dalton Trans.* **1995**, 3767.
- [32] M. G. Harris, R. Stewart, *Can. J. Chem.* **1977**, *55*, 3807.
- [33] I. B. Rother, E. Freisinger, A. Erxleben, B. Lippert, *Inorg. Chim. Acta* **2000**, *300–302*, 339.
- [34] a) A. Lebrun, R. Lavery, *Curr. Opin. Struct. Biol.* **1977**, *7*, 348 and references therein; b) D. E. Gilbert, *Curr. Opin. Struct. Biol.* **1999**, *9*, 305.
- [35] a) D. Kipling, *The Telomere*, Oxford University Press, Oxford, **1995**; b) A. I. H. Murchie, F. Aboul-Ela, G. Laughlan, B. Luisi, D. M. J. Lilley, *Nucl. Acids Mol. Biol.* **1995**, *9*, 143; c) W. I. Sundquist, *Nucl. Acids Mol. Biol.* **1991**, *5*, 1.
- [36] N. T. Thuong, C. Hélène, *Angew. Chem.* **1993**, *105*, 697; *Angew. Chem. Int. Ed. Engl.* **1993**, *32*, 666 and references therein.
- [37] See, for example: a) G. A. Leonard, S. Zhang, M. R. Peterson, S. J. Harrop, J. R. Helliwell, W. B. T. Cruse, B. d'Estainot, O. Kennard, T. Brown, W. N. Hunter, *Structure* **1995**, *3*, 335; b) S. A. Salisburg, S. E. Wilson, H. R. Powell, O. Kennard, P. Lubini, G. M. Sheldrick, N. Escaja, E. Alazzouzi, A. Grandas, E. Pedroso, *Proc. Natl. Acad. Sci. USA* **1997**, *94*, 5515; c) J. Gallego, S.-H. Chou, B. R. Reid, *J. Mol. Biol.* **1997**, *273*, 840; d) C. Cheong, R. B. Moore, *Biochemistry* **1992**, *31*, 8406; e) G. Gupta, A. E. Garcia, Q. Gua, M. Lu, N. R. Kallenbach, *Biochemistry* **1993**, *32*, 7098.
- [38] A. Kettani, A. Gorin, A. Majumdar, T. Hermann, E. Skripkin, H. Zhao, R. Jones, D. J. Patel, *J. Mol. Biol.* **2000**, *297*, 627.
- [39] a) N. Spackova, I. Berger, J. Sponer, *J. Am. Chem. Soc.* **1999**, *121*, 5519; b) N. V. Hud, F. W. Smith, F. A. L. Anet, J. Feigon, *Biochemistry* **1996**, *35*, 15383.
- [40] S. Bouaziz, A. Kettani, D. J. Patel, *J. Mol. Biol.* **1998**, *282*, 637.
- [41] a) N. Jing, R. F. Rando, Y. Pommier, M. E. Hogan, *Biochemistry* **1997**, *36*, 12498 and refs. cited therein; b) N. Jing, M. E. Hogan, *J. Biol. Chem.* **1998**, *273*, 34992.
- [42] G. B. Kauffman, D. O. Cowan, *Inorg. Synth.* **1963**, *7*, 239.
- [43] J. Arpalahti, H. Schöllhorn, U. Thewalt, B. Lippert, *Inorg. Chim. Acta* **1988**, *153*, 51.
- [44] Y. M. Chow, B. Britton, *Acta Crystallogr. Sect. B* **1975**, *31*, 1934.
- [45] W. Micklitz, B. Lippert, H. Schöllhorn, U. Thewalt, *J. Heterocyclic Chem.* **1989**, *26*, 1499.
- [46] J. S. Nowick, J. S. Chen, G. Noronha, *J. Am. Chem. Soc.* **1993**, *115*, 7636.
- [47] G. Krüger, *Hoppe Seyler's Z. Physiol. Chemie* **1894**, *18*, 434.
- [48] T. J. Kistenmacher, M. Rossi, J. P. Caradonna, L. G. Marzilli, *Adv. Mol. Relax. Interact. Processes* **1979**, *15*, 119.
- [49] G. M. Sheldrick, SHELXTL-PLUS (VMS), Siemens Analytical X-Ray Instruments, Inc.: Madison, WI, **1990**.
- [50] NONIUS BV, KappaCCD package, Röntgenweg 1, P. O.Box 811, 2600 AV Delft (Netherlands).
- [51] Z. Otwinowsky, W. Minor, *Methods Enzymol.* **1996**, *276*, 307.
- [52] G. M. Sheldrick, *Acta Crystallogr. Sect. A* **1990**, *46*, 467.
- [53] G. M. Sheldrick, SHELXL-93, Program for crystal structure refinement, University of Göttingen (Germany) **1993**.
- [54] G. M. Sheldrick, SHELXL-97, Program for the refinement of crystal structures, University of Göttingen, (Germany) **1997**.

Received: October 13, 2000 [F2796]